Mechanical Properties of Nanocrystal Supercrystals

Enrico Tam[†]*, Paul Podsiadlo*[‡]*, Elena Shevchenko*[‡]*, D. Frank Ogletree*[*]*, Marie-Paule Delplancke-Ogletree*[†]*, Paul D. Ashby*[*§]

[†]Chemicals and Materials Department, CP165/63, Université Libre de Bruxelles, Av, F.-D. Roosevelt 50, B-, 1050 Bruxelles, Belgium

[‡]Center for Nanoscale Materials, Argonne National Laboratory,9700 S. Cass Av. Argonne, IL, 60439

[*]Molecular Foundry, Lawrence Berkeley National Laboratory, 1 Cyclotron Rd., Berkeley, CA, 94720

[§]pdashby@lbl.gov

Colloidal nanocrystals attract significant interest due to their potential applications in electronic, magnetic, and optical devices. Nanocrystal supercrystals (NCSCs) are particularly appealing for their well ordered structure and homogeneity. The interactions between organic ligands that passivate the inorganic nanocrystal cores critically influence their self-organization into supercrystals. By investigating the mechanical properties of supercrystals, we can directly characterize the particle-particle interactions in a well-defined geometry, and gain insight into both the self-assembly process and the potential applications of nanocrystal supercrystals. Here we report nanoindentation studies of well ordered lead-sulfide (PbS) nanocrystal supercrystals. Their modulus and hardness were found to be similar to soft polymers at 1.7 GPa and 70 MPa respectively and the fracture toughness was 39 $KPa/m^{1/2}$, revealing the extremely brittle nature of these materials.

TOC Figure

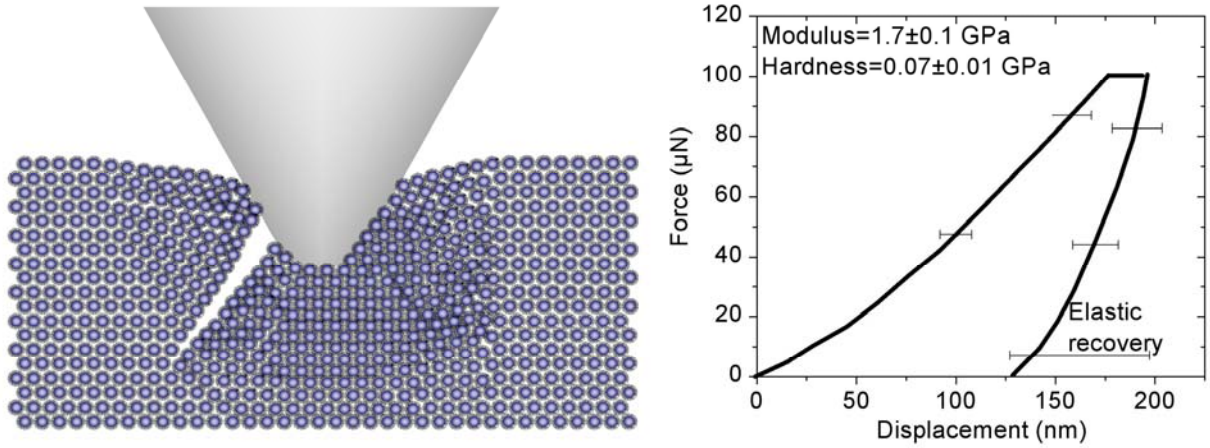
Modulus=1.7±0.1 GPa
Hardness=0.07±0.01 GPa
Force (μN)
Displacement (nm)
Elastic
recovery
0
20
40
60
80
100
120
0
50
100
150
200

Metallic and semiconductor nanocrystals are of considerable interest due to their versatile electronic and optical properties[1, 2] which can be tuned not only by changing material but also by modifying the crystal size and shape.[2-5] Similarly, mating specific properties of nanocrystals to surrounding materials can lead to functional devices. For example, Watt et. al. enhanced the efficiency of solar cells made from a PbS:MEH-PPV[1] by tuning the nanocrystal concentration and active layer thickness.[6] During solution-phase nanocrystal synthesis the inorganic cores are passivated by organic ligands. Under controlled conditions, solutions of uniform nanocrystals precipitate nanocrystal supercrystals with long-range order.[7-10] This new class of material combines the unique properties of the inorganic nanocrystal core with properties arising from the interaction between neighboring nanocrystals in the supercrystal.[3, 11] Controlling the properties of the constituent nanocrystals, ligand-particle, and ligand-ligand interactions makes it possible to further tune, direct, and optimize the NCSL properties, making supercrystals a very promising and unique material for potential applications in electronic, magnetic, and optical devices.[7, 10, 12, 13]

While optical and electronic properties of nanocrystal supercrystals have been studied and improved significantly, mechanical properties have received less attention. The range of applications of NCSL-based devices depends on NCSL mechanical properties including hardness and modulus, residual stress and strain, and fracture toughness, which underscores the importance of incorporating mechanical characterization in the design process. These properties derive from the detailed interactions between colloidal nanocrystals. These interactions are difficult to study at the single-nanocrystal level. Thus, previous mechanical studies have been reported on aggregates such as disordered electrodeposited films of colloidal CdSe nanocrystals,[14] cross-linked[15] and drop-cast[16] metal nanocrystals, and polymer-nanocrystal composites.[17, 18] Atomic force microscopy has been used to investigate the mechanical properties of ordered suspended nanocrystal sheets[12] and disordered suspended nanocrystal-polymer

---

[1] MEH-PPV is composed of 2-methoxy-5-(2'-ethyl-hexyloxy)-p-phenylene vinylene.

layers.[19] The long-range order of NCSLs provides a unique advantage. The measured bulk properties can be directly related to particle-particle interactions just as the bulk properties of normal crystals arise from the interactions between their constituent atoms.

In this letter, we report the first experimental results on the mechanical response of well-ordered three-dimensional nanocrystal supercrystals and the elucidation of their properties. The NCSLs were prepared by controllable oversaturation of a 1.5 ml chloroform solution of 7 nm PbS nanoparticles by 1.5 ml of isopropyl alcohol (a nonsolvent).[20] The nucleation of 3D colloidal crystals occurred mostly at the ITO glass immersed in the crystallization tube due to its slightly higher roughness as compared to glass walls of the crystallization tube. The crystallization process took ~3 weeks. After that, the supernatant solution was discarded and the ITO substrate with crystals was dried under house vacuum. NCSLs were ~10-200 microns in size with {111} planes parallel to the substrate (figure 1). Nanoindentation experiments were conducted with an Asylum MFP-3D™ atomic force microscope (AFM) with the low force nanoindentation accessory and Berkovich tip under load control. The optical microscope of the AFM was used to position the indenter tip over nanocrystals. The loading/unloading time was 4 seconds each, with a holding time of 4 seconds applied at the maximum load allowing creep at the beginning of the unloading phase to be less than 1 nm/s (near the drift rate of the instrument). After indentation the supercrystal surface was imaged by high resolution SEM and AFM.

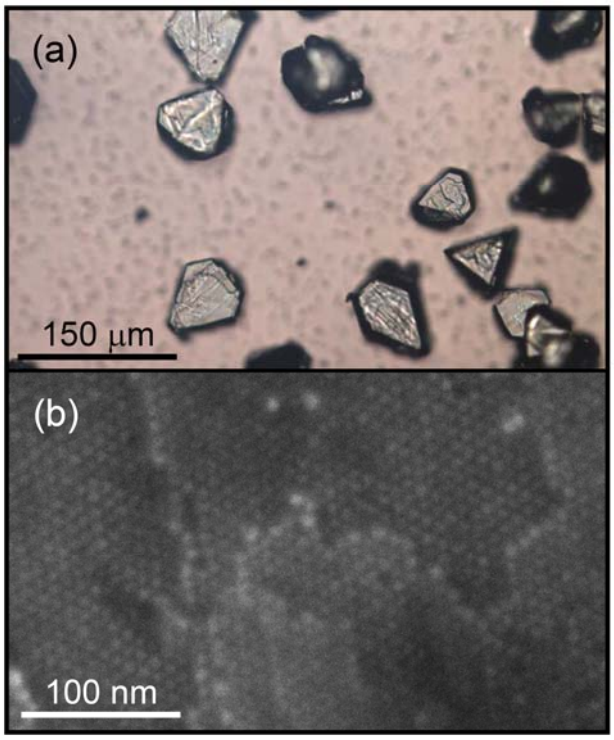

Figure 1: (a) Optical image of the highly faceted lead sulfide (PbS) nanocrystal supercrystals and (b) scanning electron microscope image of a (111) surface.

The indentation modulus and hardness were determined from the load-displacement curves by applying Oliver and Pharr analysis.[21] This method assumes that, in the absence of creep, initial unloading of the sample is elastic and the contact area stays constant, i.e. the slope of the beginning of

the unloading curve represents the stiffness of the indented material. The modulus is calculated from the stiffness and the indentation contact area inferred by the projected penetration depth and the indenter geometry. Hardness is a measure of the pressure which causes plastic deformation and is calculated by dividing the peak load during deformation by the indentation contact area. The indenter geometry was characterized by AFM imaging.

A typical load-displacement curve obtained during nanoindentation experiments on nanocrystal supercrystals is shown in figure 2a. Error bars represent the scatter of multiple measurements. In these experiments, the average modulus and hardness derived for penetrations of less than 10% of the supercrystal thickness were 1.7±0.1 and 0.07±0.01 GPa respectively. Modulus and hardness for different indentation depths are shown in Figure 1b. Hardness was found to be relatively constant for single indentations up to ~20% sample thickness. Conversely, modulus was found to increase with penetration depth. This is likely due to the indentation strain-field interacting with the high-stiffness substrate supporting the supercrystals (substrate effect). Typical practice limits the penetration depth to ~10% of the film thickness to avoid the substrate affect.[22] Nevertheless, the variation for both modulus and hardness was found to be small for penetration depths up to 20% for these supercrystal samples.

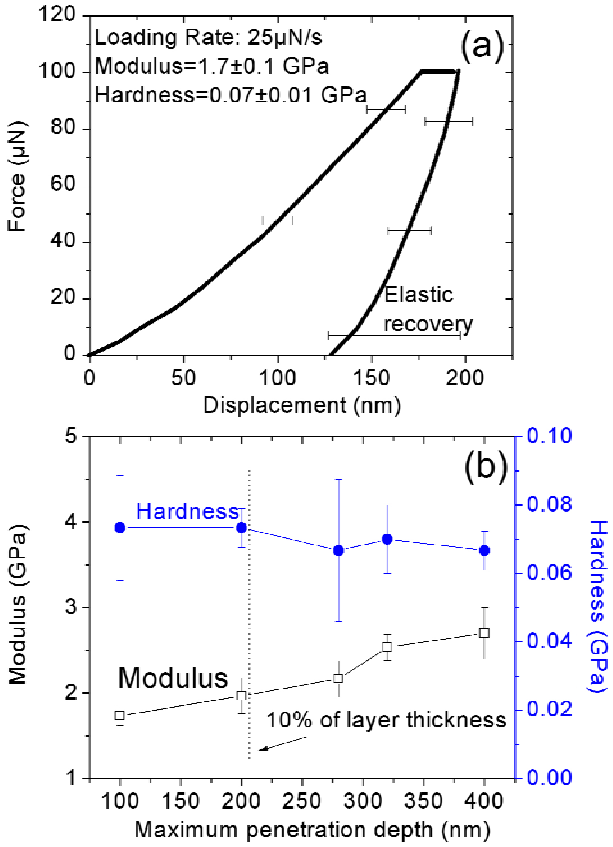

Figure 2: (a) Force vs displacement curve obtained indenting in the lead sulfide (PbS) nanocrystal supercrystals. (b) Modulus and hardness as a function of the maximum penetration depth.

The measured modulus and hardness of the nanocrystal supercrystals are more similar to organic polymers than inorganic materials. Polystyrene (PS) has a modulus of 4.3 GPa measured by nanoindentation[17] while polymethylmethacrylate (PMMA) has a modulus of 3.75 GPa and hardness of

51 MPa,[23] and different polyethelenes (PE) have modulus and hardness of 0.3-1.3 GPa and 7-18 MPa respectively.[23] Polymer nanocrystal composites are expected to show increased modulus and hardness if uniform mixing is achieved however, magnetite (Fe_3O_4) and alumina (Al_2O_3) nanoparticles did not bind well to the polymer and flocculated compromising the film's mechanical properties.[17] Cadmium Selenide (CdSe) nanocrystals using trioctylphosphineoxide (TOPO) and trioctylphosphine (TOP) as capping agents and electrodeposited into amorphous films showed a modulus of 9 GPa and hardness of 400 MPa.[14]

While the oleic acid capping agent is most similar to polyethylene chemically, the modulus and hardness of the supercrystals are like the harder plastics polystyrene and polymethylmethacrylate. The oleic acid is ~15-17 weight percent by thermogravimetric analysis (TGA) which corresponds to 40% volume fraction of oleic acid in these fcc supercrystals of PbS nanoparticles. The space filling factor for fcc crystals is 0.74 leaving 26% of the volume available to be filled by the capping agent beyond the molecules which immediately surround the inorganic cores. Assuming the inorganic core is less compliant than the organic matrix, we would expect the overall crystal stiffness to be around a factor of two greater than for pure organic material, making the polyethylene/supercrystal comparison more appropriate. The relatively high hardness may be due to the perfect packing of the supercrystal. Greater energy is required to nucleate defects than to propagate already existing defects to the boundary of the crystal.[24] Also, jamming may play an important role in this granular material. Polyethylene shows strain-hardening as the long polymer chains reorder and stretch[17], while the NCSLs with short organic ligands, as expected, do not show strain hardening.

An SEM image of a 600 μN indent (figure 3a) reveals the presence of significant cracking. Radial cracks emanate from the corners of the residual impression and lateral cracks run parallel to the edges. The relationship between the length of the radial cracks and fracture toughness for a Berkovich indenter is

$$Kc = 1.076 \cdot x_v \left(\frac{a}{l}\right)^{\frac{1}{2}} \left(\frac{E}{H}\right)^{\frac{2}{3}} \frac{P_{\max}}{c^{3/2}} \qquad (1)$$

where K_c is the fracture toughness, a is the distance from the center of the indent to the corner, l is the length of the cracks that emanate from the corners, c is the total length of the cracks, E is the modulus, H is the hardness and x_v is an empirical constant 0.015. [25-29] The measured fracture toughness was 39±3 KPa/m$^{1/2}$. Many ceramics, pure crystals,[29] and brittle polymers[30] have fracture toughness near 1 MPa/m$^{1/2}$ while clays[31] measure near 20 KPa/m$^{1/2}$, emphasizing the extremely brittle character of the nanocrystal supercrystals. Other brittle materials also show significant subsurface lateral crack formation during unloading. Crack propagation to the surface, as seen in figure 3a, could lead to "chipping".[32] The tendency toward lateral crack formation may be accentuated by the adhesion observed between the indenter and supercrystal material. Pop-in events are associated with median crack formation as radial cracks join together under the indent.[33] Although the supercrystals are very brittle, we did not observe pop-in events. This may be due to the relatively shallow indentations, since the low hardness and fracture toughness show that the material has low dissipation and surface energy. Like

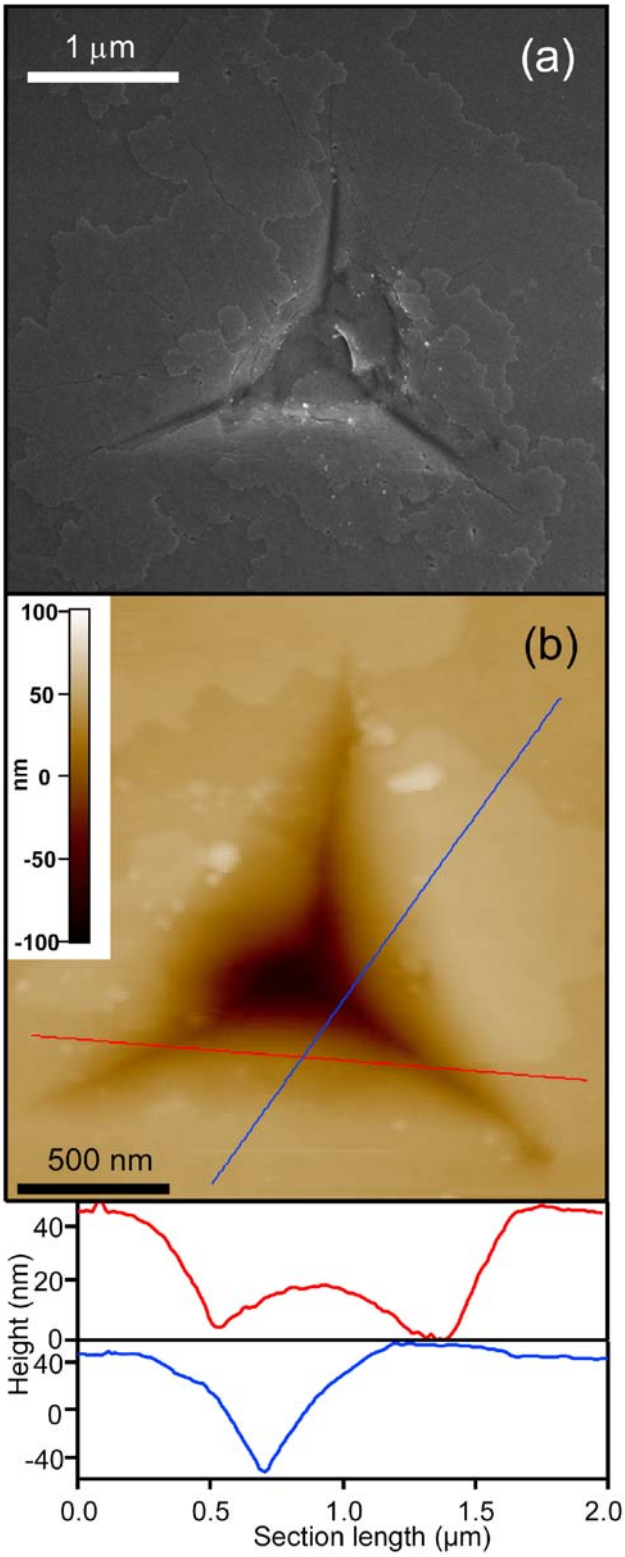

Figure 3: (a) SEM image of the residual imprint of an indentation made at a maximum load of 600μN. Radial cracks propagate from the corners of the indent and lateral cracks are parallel to the edges. (b) Atomic Force Microscopy image of a residual impression and two cross sections showing elastic recovery and no pileup.

the modulus and hardness data, the fracture toughness implicates the capping agents as the most significant factor in determining the supercrystal material properties. The extremely low fracture toughness is a result of the very weak intermolecular forces between the aliphatic capping agents and their short length which minimizes the dissipation associated with their displacement. The ease of crack propagation suggests that nanocrystal ligands are not significantly inter-digitated.

AFM and SEM images of the residual indent impression show no pile-up of displaced material at the edges of the indent (Figure 3b) thus plastic deformation significantly increases the crystal packing density. Also, stresses have been observed to grow with aging and the supercrystals tend to crack and fracture, as do amorphous nanocrystal films.[34] The development of stresses may be due to evaporation of trapped solvent or annealing of the supercrystals. Supercrystal growth requires delicate balancing of interparticle energies to avoid amorphous film formation. The local structure of the capping ligands may be in an extended, kinetically-trapped state resulting from condensation into the supercrystal followed by solvent evaporation. The existence of such metastable states is consistent with the significant creep observed during the holding period after loading, as well as the densification of the NCSL during indentation. The values of modulus, hardness, and fracture toughness presented herein could be underrepresented due to these stresses compared to the relaxed material's properties. The error is unlikely to be significant and does not influence the scientific conclusions of our analysis.

The chemical composition of the capping agents clearly determines the mechanical properties of the supercrystals. Oleic acid's short chain length and mostly-saturated character lead to very weak intermolecular forces which result in marked plasticity and brittleness. The very low fracture toughness causes the NCSL to fracture under their own or with slight stress. To improve the supercrystal mechanical properties requires different capping agents with stronger intermolecular forces or posts-preparative modifications such as annealing or plasma treatment.[35]

This work constitutes the first measurement of the mechanical properties of PbS nanocrystal supercrystals. Elastic modulus and hardness measured 1.7±0.1 and 0.07±0.01, respectively which is quite similar to soft polymers. The weak fracture toughness of ~ 39±3 $KPa/m^{1/2}$ gives colloidal crystal

clay-like behavior. The capping molecules seems to significantly impact the mechanical properties and hence their smart design is required to improve the material strength.

Acknowledgment

Work at the Molecular Foundry and Center for Nanoscale Materials were supported by the Office of Science, Office of Basic Energy Sciences, of the U.S. Department of Energy under Contract No. DE-AC02-05CH11231 and DE-AC02-06CH11357 respectively. E. T. was supported by an ARC Project of the French Community of Belgium.

References

1. Colvin, V. L.; Schlamp, M. C.; Alivisatos, A. P., Light-emitting diodes made from cadmium selenide nanocrystals and a semiconducting polymer. *Nature* **1994,** 370, (6488), 354-357.
2. Klein, D. L.; Roth, R.; Lim, A. K. L.; Alivisatos, A. P.; McEuen, P. L., A single-electron transistor made from a cadmium selenide nanocrystal. *Nature* **1997,** 389, (6652), 699-701.
3. Collier, C. P.; Saykally, R. J.; Shiang, J. J.; Henrichs, S. E.; Heath, J. R., Reversible Tuning of Silver Quantum Dot Monolayers Through the Metal-Insulator Transition. *Science* **1997,** 277, (5334), 1978-1981.
4. Duan, T.; Lou, W.; Wang, X.; Xue, Q., Size-controlled synthesis of orderly organized cube-shaped lead sulfide nanocrystals via a solvothermal single-source precursor method. *Colloids and Surfaces A: Physicochemical and Engineering Aspects* **2007,** 310, (1-3), 86-93.
5. He, J.; Liu, C.; Li, F.; Sa, R.; Wu, K., Size-dependence of stability and optical properties of lead sulfide clusters. *Chemical Physics Letters* **2008,** 457, (1-3), 163-168.
6. Watt, A. A. R.; Blake, D.; Warner, J. H.; Thomsen, E. A.; Tavenner, E. L.; Rubinsztein-Dunlop, H.; Meredith, P., Lead sulfide nanocrystal: conducting polymer solar cells. *Journal of Physics D: Applied Physics* **2005,** 38, (12), 2006-2012.
7. Murray, C. B.; Kagan, C. R.; Bawendi, M. G., Self-Organization of CdSe Nanocrystallites into Three-Dimensional Quantum Dot Supercrystals. *Science* **1995,** 270, (5240), 1335-1338.
8. Shevchenko, E. V.; Talapin, D. V.; Kotov, N. A.; O'Brien, S.; Murray, C. B., Structural diversity in binary nanoparticle supercrystals. *Nature* **2006,** 439, (7072), 55-59.
9. Shevchenko, E. V.; Talapin, D. V.; O'Brien, S.; Murray, C. B., Polymorphism in AB13 Nanoparticle Supercrystals: An Example of Semiconductor−Metal Metamaterials. *Journal of the American Chemical Society* **2005,** 127, (24), 8741-8747.
10. Sun, S.; Murray, C. B.; Weller, D.; Folks, L.; Moser, A., Monodisperse FePt Nanoparticles and Ferromagnetic FePt Nanocrystal Supercrystals. *Science* **2000,** 287, (5460), 1989-1992.
11. Kagan, C. R.; Murray, C. B.; Bawendi, M. G., Long-range resonance transfer of electronic excitations in close-packed CdSe quantum-dot solids. *Physical Review B* **1996,** 54, (12), 8633.
12. Mueggenburg, K. E.; Lin, X.-M.; Goldsmith, R. H.; Jaeger, H. M., Elastic membranes of close-packed nanoparticle arrays. *Nat Mater* **2007,** 6, (9), 656-660.
13. Urban, J. J.; Talapin, D. V.; Shevchenko, E. V.; Kagan, C. R.; Murray, C. B., Synergism in binary nanocrystal supercrystals leads to enhanced p-type conductivity in self-assembled PbTe/Ag2Te thin films. *Nat Mater* **2007,** 6, (2), 115-121.

14. Lee, D.; Jia, S.; Banerjee, S.; Bevk, J.; Herman, I. P.; Kysar, J. W., Viscoplastic and Granular Behavior in Films of Colloidal Nanocrystals. *Physical Review Letters* **2007,** 98, (2), 026103-4.
15. Klajn, R.; Bishop, K. J. M.; Fialkowski, M.; Paszewski, M.; Campbell, C. J.; Gray, T. P.; Grzybowski, B. A., Plastic and Moldable Metals by Self-Assembly of Sticky Nanoparticle Aggregates. *Science* **2007,** 316, (5822), 261-264.
16. Raichman, Y.; Kazakevich, M.; Rabkin, E.; Tsur, Y., Inter-Nanoparticle Bonds in Agglomerates Studied by Nanoindentation. *Advanced Materials* **2006,** 18, (15), 2028-2030.
17. Ciprari, D.; Jacob, K.; Tannenbaum, R., Characterization of Polymer Nanocomposite Interphase and Its Impact on Mechanical Properties. *Macromolecules* **2006,** 39, (19), 6565-6573.
18. Song, H. M.; Kim, Y. J.; Park, J. H., Three-Dimensional Hierarchically Organized Magnetic Nanoparticle Polymer Composites: Achievement of Monodispersity and Enhanced Tensile Strength. *The Journal of Physical Chemistry C* **2008,** 112, (14), 5397-5404.
19. Markutsya, S.; Jiang, C.; Pikus, Y.; Tsukruk, V. V., Freely Suspended Layer-by-Layer Nanomembranes: Testing Micromechanical Properties. *Advanced Functional Materials* **2005,** 15, (5), 771-780.
20. Shevchenko, E.; Talapin, D.; Kornowski, A.; Wiekhorst, F.; Kötzler, J.; Haase, M.; Rogach, A.; Weller, H., Colloidal Crystals of Monodisperse FePt Nanoparticles Grown by a Three-Layer Technique of Controlled Oversaturation. *Advanced Materials* **2002,** 14, (4), 287-290.
21. Oliver, W. C.; Pharr, G. M., An improved technique for determining hardness and elastic modulus using load and displacement sensing indentation experiments were. *Journal of Materials Research* **1992,** 7, (6), 1564-1583.
22. Chudoba, T.; Schwarzer, N.; Richter, F., Determination of elastic properties of thin films by indentation measurements with a spherical indenter. *Surface and Coatings Technology* **2000,** 127, (1), 9-17.
23. Klapperich, C.; Komvopoulos, K.; Pruitt, L., Nanomechanical Properties of Polymers Determined From Nanoindentation Experiments. *Journal of Tribology* **2001,** 123, (3), 624-631.
24. Shan, Z. W.; Mishra, R. K.; Syed Asif, S. A.; Warren, O. L.; Minor, A. M., Mechanical annealing and source-limited deformation in submicrometre-diameter Ni crystals. *Nat Mater* **2008,** 7, (2), 115-119.
25. Palmqvist, S., A method to determine the toughness of brittle materials, especially hard materials. *Jenkontorets Ann.* **1957,** 141, 300-307.
26. Laugier, M. T., The elastic/plastic indentation of ceramics. *Journal of Materials Science Letters* **1985,** 4, (12), 1539-1541.
27. Laugier, M. T., Palmqvist indentation toughness in WC-Co composites. *Journal of Materials Science Letters* **1987,** 6, (8), 897-900.
28. Ouchterlony, F., Stress intensity factors for the expansion loaded star crack. *Engineering Fracture Mechanics* **1976,** 8, (2), 447-448.
29. Rodney D. Dukino, M. V. S., Comparative Measurement of Indentation Fracture Toughness with Berkovich and Vickers Indenters. *Journal of the American Ceramic Society* **1992,** 75, (12), 3299-3304.
30. Callister, W. D., *Materials Science and Engineering: An introduction*. John Wiley and Sons, Inc.: New York, New York, 1994.
31. Wang, J.-J.; Zhu, J.-G.; Chiu, C. F.; Zhang, H., Experimental study on fracture toughness and tensile strength of a clay. *Engineering Geology* **2007,** 94, (1-2), 65-75.
32. Lawn, B. R.; Swain, M. V.; Phillips, K., On the mode of chipping fracture in brittle solids. *Journal of Materials Science* **1975,** 10, (7), 1236-1239.
33. Field, J. S.; Swain, M. V.; Dukino, R. D., Determination of fracture toughness from the extra penetration produced by indentation-induced pop-in. *Journal of Materials Research* **2003,** 18, (6), 1412-1419.

34. Jia, S.; Banerjee, S.; Lee, D.; Bevk, J.; Kysar, J. W.; Herman, I. P., Fracture in electrophoretically deposited CdSe nanocrystal films. *Journal of Applied Physics* **2009,** 105, (10), 103513-9.
35. Cademartiri, L.; Bertolotti, J.; Sapienza, R.; Wiersma, D. S.; von Freymann, G.; Ozin, G. A., Multigram Scale, Solventless, and Diffusion-Controlled Route to Highly Monodisperse PbS Nanocrystals. *The Journal of Physical Chemistry B* **2005,** 110, (2), 671-673.